Demonstration of Fidelity Improvement Using Dynamical Decoupling with Superconducting Qubits

Bibek Pokharel,[1,*] Namit Anand,[2] Benjamin Fortman,[3] and Daniel A. Lidar[1,2,3,4]
[1]*Department of Electrical Engineering, University of Southern California, Los Angeles, California 90089, USA*
[2]*Department of Physics and Astronomy, University of Southern California, Los Angeles, California 90089, USA*
[3]*Department of Chemistry, University of Southern California, Los Angeles, California 90089, USA*
[4]*Center for Quantum Information Science & Technology, University of Southern California, Los Angeles, California 90089, USA*

(Received 4 August 2018; published 29 November 2018)

Quantum computers must be able to function in the presence of decoherence. The simplest strategy for decoherence reduction is dynamical decoupling (DD), which requires no encoding overhead and works by converting quantum gates into decoupling pulses. Here, using the IBM and Rigetti platforms, we demonstrate that the DD method is suitable for implementation in today's relatively noisy and small-scale cloud-based quantum computers. Using DD, we achieve substantial fidelity gains relative to unprotected, free evolution of individual superconducting transmon qubits. To a lesser degree, DD is also capable of protecting entangled two-qubit states. We show that dephasing and spontaneous emission errors are dominant in these systems, and that different DD sequences are capable of mitigating both effects. Unlike previous work demonstrating the use of quantum error correcting codes on the same platforms, we make no use of postselection and hence report unconditional fidelity improvements against natural decoherence.

DOI: 10.1103/PhysRevLett.121.220502

Introduction.—Two decades after the first detailed quantum computing proposals [1–4], rudimentary gate-model quantum computers (QCs) based on superconducting transmon qubits with coherence times in the microsecond range are finally available and remotely accessible via public cloud-based services. Interest in these platforms, made publicly available so far by IBM, Rigetti, and Alibaba, has been high, and numerous experiments have been reported demonstrating a variety of quantum protocols [5–8] and algorithms [9–11]. Given their present intermediate scale of 10–20 fairly noisy qubits, gates, and measurements [12], the current QCs are particularly very well suited to tests of simple quantum error correction and suppression protocols. Indeed, a variety of quantum error correction (QEC) experiments on cloud-based platforms have been reported [13–19]. However, so far this body of work has not offered a demonstration that QEC can result in improvements for general decoherence while applying standard initialization, gates, and readout operations (we review these studies in Ref. [20], Sec. A). The main reason appears to be that the overhead introduced by QEC results in error rates that are too high to be compensated by the schemes that have been tried so far, and claims of improvement have had to resort to cleverly avoiding the execution of actual initialization and key gate operations [19].

Here, rather than attempting to demonstrate error correction, we focus on error suppression. Specifically, we seek to mitigate the effects of decoherence using dynamical decoupling (DD) [36–39], one of the simplest strategies available in the toolkit of quantum error mitigation [40]. We demonstrate that DD is capable of extending the lifetimes of single-qubit states as well as entangled two-qubit states. To the best of our knowledge, this amounts to the first unequivocal demonstration of successful decoherence mitigation in cloud-based superconducting qubit platforms. Moreover, as a test of the robustness of our results we performed DD experiments on three of the cloud-based systems, the 16-qubit IBMQX5, 5-qubit IBMQX4, and the 19-qubit Rigetti Acorn chips. Given their similarities they provide suitable platforms for independent tests of the performance of DD and we expect that the lessons drawn will have wide applicability.

Dynamical decoupling.—DD is a well-established method designed to suppress decoherence via the application of pulses applied to the system, that cancel the system-environment interaction to a given order in time-dependent perturbation theory [41]. A large variety of DD protocols has been developed and tested, with some of the more advanced protocols capable of reducing decoherence to arbitrarily low levels under the assumption of perfectly implemented instantaneous pulses with arbitrarily small pulse intervals [42–46]. In reality, pulses are of course never implemented perfectly, have a minimum duration, and pulse intervals are finite. Various specialized DD sequences have been developed to handle such conditions as well [34,47–50] and it has been shown that imperfect DD can improve the performance of fault-tolerant quantum computation [51]. Here, as a proof of principle, we explore

the benefits of using primarily the simplest DD sequence, designed to offer only first order cancellation and not designed with robustness against pulse imperfections in mind, namely, the $XY4$ "universal decoupling" sequence [39]. This sequence consists of a simple repetition of the pulse pattern $XYXY$, where X and Y are rotations by π about the x and y axes of the single-qubit Bloch sphere, and the system evolves freely for time τ between the pulses. Starting from the system-bath Hamiltonian $H = H_S + H_B + H_{\rm SB}$, with the interaction term $H_{\rm SB} = \sum_{i=1}^{N} \sum_{\alpha\in\{x,y,z\}} \sigma_i^\alpha \otimes B_i^\alpha$, where σ_i^α and B_i^α are, respectively, Pauli matrices acting on qubit i, and general operators acting on the bath, the action of the $XY4$ sequence is readily shown to result in the elimination of $H_{\rm SB}$ to first order in τ in the joint system-bath unitary propagator, under the assumption of instantaneous X and Y pulses.

Methodology.—The native single gates on the IBM and Rigetti platforms are rotations $R_\alpha(\phi) = \exp[i(\phi/2)\sigma^\alpha]$, with $\alpha \in \{y, z\}$ (see Ref. [20], Sec. B, for more details about these platforms). Arbitrary single-qubit unitaries can be applied by specifying Euler angles θ, ϕ, λ such that $U(\theta, \phi, \lambda) = iR_z(\phi)R_y(\theta)R_z(\lambda)$. Since DD is expected to provide quantum error suppression for arbitrary initial states, we tested the performance of DD on a variety of initial states by repeatedly preparing single-qubit states of the form $|\psi\rangle = U(\theta, \phi, \lambda)|0\rangle$, where $|0\rangle$ and $|1\rangle$ are computational basis states (eigenstates of σ^z). It should be noted that in transmon qubits the $|0\rangle$ and $|1\rangle$ states are, respectively, the ground and first excited states; this has important implications as discussed below. DD pulses were applied as the gates $X = i\exp[-i(\pi/2)\sigma^x] = U(\pi, 0, \pi)$ and $Y = i\exp[-i(\pi/2)\sigma^y] = U(\pi, 2\pi, 0)$. On the IBMQX5 (Acorn) chip each single-qubit pulse lasted 80 (40) ns, with a 10 ns buffer of free evolution between pulses, and each such run was repeated 8192 (1000) times. Identity pulses were implemented as free evolutions lasting 90 (50) ns on the IBMQX5 (Acorn) chip. Since measurements are only possible in the Z basis, we applied $U^\dagger(\theta, \phi, \lambda)$ at the end of each run and measured the final state of each qubit in the Z basis.

Our key performance metric is the fidelity between the input and the output states, defined as the total number of $|0\rangle$ states empirically observed divided by the total number of repetitions. We considered two types of initial conditions. In "type 1," θ was varied in 16 equidistant steps in the range $[0, \pi]$, with $\phi = \lambda = 0$. This corresponds to a sequence of states (superpositions for $0 < \theta < \pi$) of the form $|\psi\rangle = \cos(\theta/2)|0\rangle + \sin(\theta/2)|1\rangle$ (up to a global phase). In "type 2," we considered a set of 30 random initial conditions sampled uniformly from the Bloch sphere along with the 6 eigenstates of the Pauli matrices, i.e., $|0\rangle, |1\rangle, |\pm\rangle = (1/\sqrt{2})(|0\rangle \pm |1\rangle), |\pm i\rangle = (1/\sqrt{2})(|0\rangle \pm i|1\rangle)$.

Single-qubit results.—We first tested the dependence on the initial state using type 1 preparation, as shown in Fig. 1. Under free evolution, the fidelity is relatively high for $\theta \approx 0$ (corresponding to the ground state $|0\rangle$) on both devices, and approaches a clear minimum for $\theta \approx (5\pi/8)$, i.e., a superposition state slightly biased towards $|1\rangle$. On both devices the free evolution fidelity rises towards the excited state $|1\rangle$, but remains well below that of the ground state. Thus coherent superposition states undergo significant dephasing and the excited state $|1\rangle$ undergoes spontaneous emission (SE) and relaxes to the ground state.

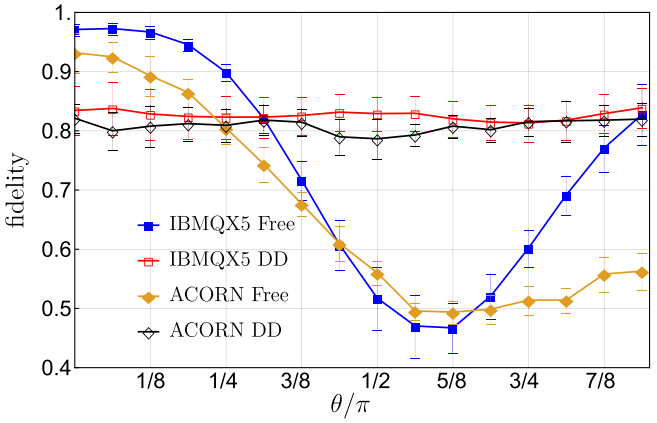

FIG. 1. Mean fidelity over 16 qubits of IBMQX5 and 15 qubits of Acorn, for initial states $|\psi\rangle = -i[\cos(\theta/2)|0\rangle + \sin(\theta/2)|1\rangle]$. Results shown are under DD using XY4 and under free evolution. IBMQX5: after $N = 40$ pulses, i.e., 10 repetitions of the base $XY4$ sequence. DD improves the fidelity only for states with $\theta \gtrsim \pi/3$. Acorn: after $N = 192$ pulses, i.e., 48 repetitions of the base $XY4$ sequence. DD improves the fidelity only for states with $\theta \gtrsim \pi/4$. Throughout, we report 2σ error bars (95% confidence intervals) calculated using the bootstrap method (for more details see Ref. [20], Sec. C).

The situation is dramatically different under DD. When compared at the pulse number for which DD exhibits the highest error suppression [$N = 40$ (192) for IBM (Rigetti)], on both devices the θ dependence is essentially eliminated, as shown in Fig. 1. It is clear that the overall fidelity (averaged over θ) increases significantly, while DD reduces the fidelity of states close to the ground state. This is consistent with the $XY4$ sequence suppressing all single-qubit error types equally. For more details see Ref. [20], Sec. D.

Figure 2 shows the results under type 2 preparation. For IBMQX5, DD significantly reduces the fidelity decay up to $N \approx 110$ pulses. The free evolution fidelity decays rapidly but has a shallow minimum at $N \approx 60$, then surpasses the fidelity under DD for $N > 110$, which continues to decay exponentially. This exponential decay is consistent with Markovian dynamics.

The situation is rather different for Acorn. First, we note that the initial fidelity (determined by the initialization and readout errors) is lower for Acorn than for IBMQX5: ~0.91 and ~0.96, respectively. Second, the fidelity under DD is consistently greater than under free evolution, and the roles are reversed: free evolution is very nearly Markovian

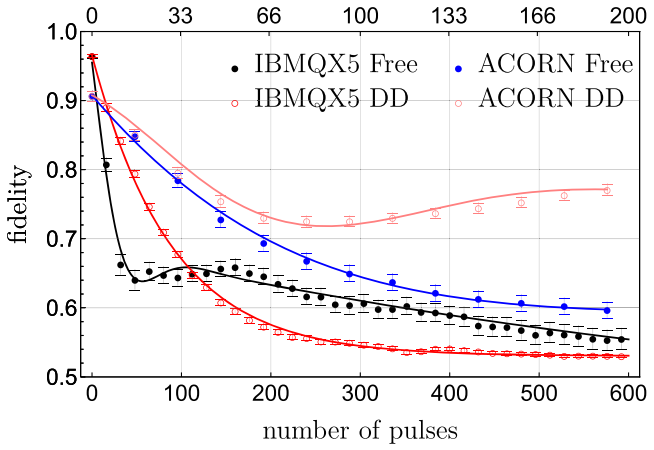

FIG. 2. Mean fidelity, after averaging over all qubits, and all 36 initial conditions in type 2 preparation, as a function of the number of pulses for IBMQX5 (bottom axis) and Acorn (top axis). The pulse interval is the shortest possible: 90 ns for IBMQX5, and 50 ns for Acorn. Solid lines are fits to Eq. (1), with fit parameters as per Table I.

(exponential decay) while under DD it exhibits a recurrence. These fidelity differences suggest that the environments are different for the two QCs, with the native IBMQX5 environment being non-Markovian, while that of Acorn is more Markovian. Conversely, DD removes the non-Markovian component for IBMQX5, while it introduces a non-Markovian component for Acorn. We may speculate that the non-Markovianity is due to residual low-frequency noise (e.g., $1/f$) in the IBMQX5 case, and that the DD pulses themselves introduce low frequency noise in the Acorn case.

To quantify the fidelity decay with and without DD we fit the data to a modulated exponential decay with three free parameters λ, α (dimensionless decay times), and γ (dimensionless modulation frequency):

$$F(N) = cf(N) + c_0, \qquad f(N) = e^{-N/\lambda}\cos(N\gamma) + e^{-N/\alpha}.$$
$$c = \frac{F_{N_{\max}} - F_0}{f(N_{\max}) - 1}, \qquad c_0 = F_0 - c. \tag{1}$$

Here, F_0 is the initial fidelity, $F_{N_{\max}}$ is the fidelity at $N =$ 592 (192) for IBMQX5 (Acorn). The deviation of $F_{N_{\max}}$ from 1 accounts for the initialization errors, readout errors, and decoherence that were not canceled by DD, as well as the errors accumulated during the application of the imperfect DD pulses, arising from imperfect control over the pulse shape, duration, and interval. Table I summarizes the values of the fit parameters.

While λ quantifies the sharp decay during the beginning of the evolution, evolution at longer timescales is quantified by α. The most significant finding for IBMQX5 is that the initial decay time characterized by λ is more than tripled in the presence of DD. While the improvement in decay time is much more modest for Acorn, the result is in a sense even better than for IBMQX5, in that DD improves its fidelity for *all* N we were able to test. We also tested DD on the 5-qubit IBMQX4, with similar results (see Ref. [20], Sec. B. 2, for details).

Dephasing vs spontaneous emission.—Figure 1 shows that both dephasing and SE play important roles. This is studied in more detail in Ref. [20], Sec. D, where we show that for initial states close to the ground state $|0\rangle$, DD is worse than free evolution, but for superposition states susceptible to dephasing, and states close to the excited state $|1\rangle$ susceptible to SE, there is a clear benefit in using the $XY4$ sequence. In light of this, it is interesting to try to address one of these error sources at a time. A DD sequence that suppresses only dephasing (σ^z) errors is $(XI)^N$ or $(YI)^N$ (N repetitions of XI or YI), since X and Y anticommute with σ^z. Likewise, SE is suppressed by $(ZI)^N$, since Z anticommutes with σ^-. We report on results for these sequences in Ref. [20], Sec. E; they underperform $XY4$, as expected, but both lead to a substantial slowing down of fidelity decay, with dephasing suppression being the dominant effect, accounting for nearly 90% of the value of λ under $XY4$. This can be viewed as an example of using DD as a diagnostic tool, to identify the relative dominance of different decoherence channels [52,53].

Dependence on the pulse interval.—It is well known from DD theory that performance depends strongly on the pulse interval τ [40]. We thus consider the intersection time of the fidelity curves under free evolution and DD for IBMQX5, denoted t_{int}, which represents the duration over which DD improves the fidelity over free evolution. The dependence on τ is shown in Fig. 3. We observe that, as

TABLE I. Fit parameters when Eq. (1) is used to fit the mean fidelities in Fig. 2. The first decay constant λ is significantly increased under DD. The second decay constant α is effectively infinite for all evolutions other than IBMQX5's free evolution. The modulation frequency γ vanishes for IBMQX5 under DD and is near zero for Acorn under free evolution, consistent with purely exponential fidelity decay, i.e., Markovian evolution.

Machine	Evolution	$F_0 \times 10^{-2}$	$F_{N_{\max}} \times 10^{-2}$	λ	α	γ
IBMQX5	Free	96.5 ± 0.1	55.6 ± 0.7	28.9 ± 1.2	910 ± 5	0.73 ± 0.12
IBMQX5	DD	96.5 ± 0.1	53.1 ± 0.1	88.4 ± 0.3	∞	0
Acorn	Free	90.8 ± 0.4	59.8 ± 0.6	68.1 ± 1.3	∞	0.14 ± 0.11
Acorn	DD	90.8 ± 0.4	77.1 ± 0.4	74.9 ± 0.9	∞	$0.50 \pm .03$

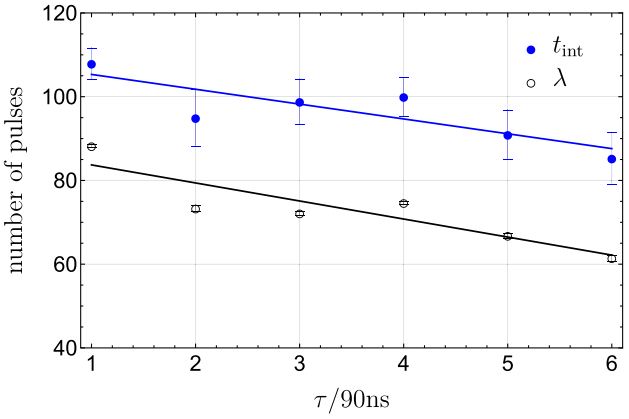

FIG. 3. DD performance as a function of pulse interval τ for IBMQX5 (in units of 90 ns). The intersection time $t_{\rm int}$ of the fidelity curves under free evolution and DD, and the decay-time exponent λ, as a function of the pulse spacing τ. Linear fits yield $t_{\rm int} = -3.5(\tau/90\ \text{ns}) + 108$ and $\lambda = -4.3(\tau/90\ \text{ns}) + 88.0$.

expected, $t_{\rm int}$ decays to first order in τ, implying that as the pulse interval increases, DD becomes less effective. Also shown in Fig. 3 is the decay-time exponent λ as a function of τ, which behaves similarly: λ decays from an initial value of ≈88 to ≈60, still twice as large as that of free evolution (≈29). Somewhat surprisingly, both $t_{\rm int}$ and λ decay nonmonotonically with τ, a finding that is not captured by standard DD theory and presents an interesting open theoretical problem. Additional analysis is presented in Ref. [20], Sec. F.

Protection of two-qubit entangled states.—To evaluate the performance of DD in preserving entangled states, we initialized qubit pairs in Bell states of the form $|\Phi^+\rangle = (1/\sqrt{2})(|00\rangle + |11\rangle)$ and $|\Psi^+\rangle = (1/\sqrt{2})(|01\rangle + |10\rangle)$, followed by an $XY4$ DD sequence (higher order DD sequences for entanglement protection are known as well [54]). Ideally, one would perform the measurements in the Bell basis and report the corresponding fidelities. However, we found that due to the relatively large errors introduced by CNOT gates and the high readout errors, Bell basis measurements yielded very noisy data which was difficult to draw meaningful conclusions from. Therefore we instead performed a measurement of both qubits in the computational basis $\{|00\rangle, |01\rangle, |10\rangle, |11\rangle\}$.

Let p_{ij} be the probability of measuring the computational basis state $|ij\rangle$, with $i, j \in \{0, 1\}$. Our results are plotted in Fig. 4, which shows the probabilities p_{ij} that were measured after initializing the system in a Bell state and letting it evolve either freely or under DD. Under ideal conditions one would expect to have $p_{00} = p_{11} = 0.5$ for $|\Phi^+\rangle$ and $p_{01} = p_{10} = 0.5$ for $|\Psi^+\rangle$. Instead, for both QCs, Fig. 4 (top row) shows a strong bias for $|00\rangle$ over $|11\rangle$ upon initialization ($N = 0$) for the $|\Phi^+\rangle$ case, with some contamination by the $|01\rangle$ and $|10\rangle$ states. For the $|\Psi^+\rangle$ case, Fig. 4 (bottom row) shows contamination by $|00\rangle$ and $|11\rangle$ upon initialization (stronger for IBMQX5 than for Acorn), and a curious bias towards $|01\rangle$ over $|10\rangle$ for Acorn. We attribute these effects to the single-digit percentage readout errors (see Ref. [20], Sec. B) and the CNOT gate errors. Clearly, the preparation of the Bell states is itself prone to substantial errors on both QCs.

As mentioned earlier, SE plays a key role and, consequently, the main effect under free evolution is a sharp increase in p_{00} with N on both devices. Under DD, the main beneficial effect is that this dominance of the ground state $|00\rangle$ is suppressed. However, on IBMQX5 for both $|\Phi^+\rangle$ and $|\Psi^+\rangle$ a nearly uniform distribution over all four

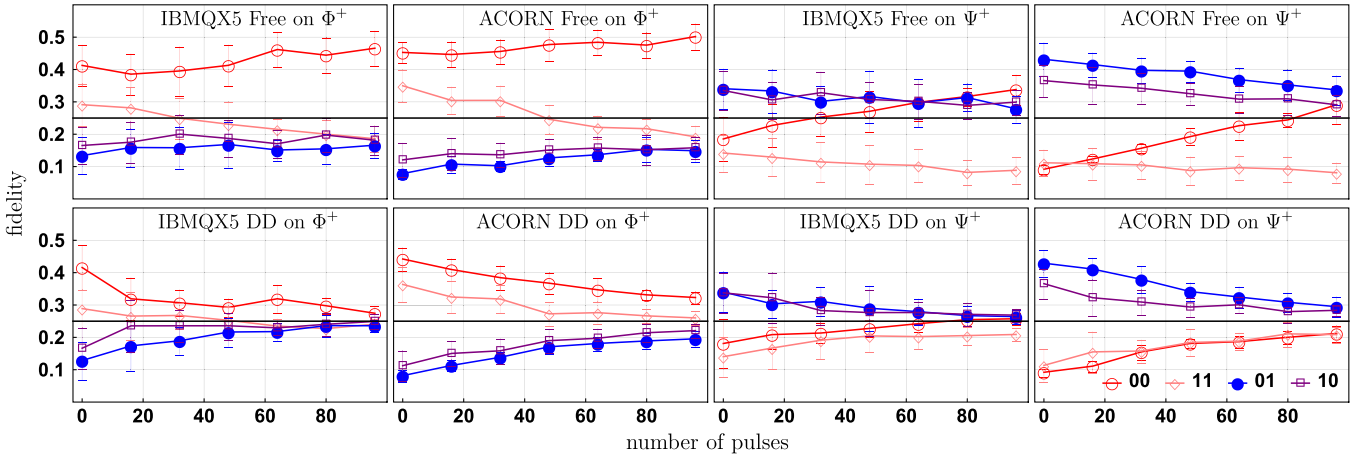

FIG. 4. Probabilities of different computational basis states after DD for initially prepared Bell states $|\Phi^+\rangle = (1/\sqrt{2})(|00\rangle + |11\rangle)$ and $|\Psi^+\rangle = (1/\sqrt{2})(|01\rangle + |10\rangle)$, as a function of the number of pulses, for both IBMQX5 and Acorn. Top row: free evolution. Bottom row: evolution under DD. The $|00\rangle$ state is favored under free evolution. The solid horizontal line indicates $p = 0.25$, the limit of a fully mixed state. For $|\Psi^+\rangle$ there is no noticeable difference in the performance with or without DD. For $|\Phi^+\rangle$ on IBMQX5, after $N \approx 20$, $p_{11} \approx 0.25$, suggesting that at this point all information has essentially been scrambled. On Acorn, complete scrambling of $|\Phi^+\rangle$ occurs after $N \sim 30$. Overall, DD is more effective at slowing down the decay to the fully mixed state for Acorn than for IBMQX5.

computational basis states is reached after 100 pulses. The trend is similar for Acorn, but the decay to the fully mixed state is slowed down more by DD than for IBMQX5, and DD manages to keep the original ratio of p_{00}/p_{11} up to ~50 pulses. Overall, it is clear that entanglement is rapidly lost, but is slowed down somewhat by DD.

Conclusions and outlook.—Our results demonstrate the undeniable usefulness of DD on prototype QCs for the suppression of inherent decoherence, a feature which has yet to be demonstrated unconditionally using QEC [13–19] (see Ref. [20], Sec. A). It is remarkable that performance improvement was achievable despite significant pulse implementation imperfections. Therefore, we conclude that, given a quantum circuit, it is already advantageous to perform dynamically decoupled evolution rather than free evolution between computational gates [51].

In the future, as the error rates of measurement and multiqubit gates are reduced, it should become possible to more accurately assess the effectiveness of DD. We anticipate that reduction in multiqubit errors will alleviate the restrictions placed by connectivity of the qubits as it will be possible to perform more SWAP gates without corrupting the states. In such scenarios, hybrid QEC-DD [51,55,56] methods could be experimentally assessed and would constitute an attractive near-term target for higher performance gains than is enabled by either scheme alone.

Another attractive prospect for future experiments is the implementation of higher-order DD sequences. Indeed, we have already tested higher-order sequences based on genetic algorithms [34], and found a small improvement over *XY*4 (see Ref. [20], Sec. G). The success of such sequences in providing better fidelity improvements than the XY4 sequence will depend on improved pulse control (such as the ability to fine-tune pulse intervals, needed to implement UDD [43] and QDD [44]), reduction of the pulse interval and duration, etc. Implementation of robust DD sequences [34,47–50] is another particularly promising venue.

We acknowledge the use of the IBM Quantum Experience and Rigetti's Forest for this work. The views expressed are those of the authors and do not reflect the official policy or position of IBM, the IBM Quantum Experience team, Rigetti, or the Rigetti team. This work was supported in part by Oracle Labs, part of Oracle America, Inc. which provided the funding for the donation in support of this academic research. Financial support from the Lockheed Martin Corporation is gratefully acknowledged. We are grateful to Haimeng Zhang for insightful discussions.

*Corresponding author.
pokharel@usc.edu.

[1] J. I. Cirac and P. Zoller, Phys. Rev. Lett. **74**, 4091 (1995).
[2] D. Loss and D. P. DiVincenzo, Phys. Rev. A **57**, 120 (1998).
[3] B. E. Kane, Nature (London) **393**, 133 (1998).
[4] Y. Nakamura, Y. A. Pashkin, and J. S. Tsai, Nature (London) **398**, 786 (1999).
[5] D. Alsina and J. I. Latorre, Phys. Rev. A **94**, 012314 (2016).
[6] M. Berta, S. Wehner,, and M. M. Wilde, New J. Phys. **18**, 073004 (2016).
[7] S. Das and G. Paul, arXiv:1712.04925.
[8] S. Deffner, Heliyon **3**, e00444 (2017).
[9] D. Ristè, M. P. da Silva, C. A. Ryan, A. W. Cross, A. D. Córcoles, J. A. Smolin, J. M. Gambetta, J. M. Chow, and B. R. Johnson, Quantum Inf. **3**, 16 (2017).
[10] R. Li, U. Alvarez-Rodriguez, L. Lamata, and E. Solano, Quantum Meas. Quantum Metrol. **4**, 1 (2017).
[11] P. J. Coles *et al.*, arXiv:1804.03719.
[12] J. Preskill, Quantum **2**, 79 (2018).
[13] S. J. Devitt, Phys. Rev. A **94**, 032329 (2016).
[14] J. R. Wootton and D. Loss, Phys. Rev. A **97**, 052313 (2018).
[15] C. Vuillot, Quantum Inf. Comput. **18**, 0949 (2018).
[16] J. Roffe, D. Headley, N. Chancellor, D. Horsman, and V. Kendon, Quantum Sci. Technol. **3**, 035010 (2018).
[17] I. K. Sohn, S. Tarucha,, and B.-S. Choi, Phys. Rev. A **95**, 012306 (2017).
[18] D. Willsch, M. Nocon, F. Jin, H. De Raedt, and K. Michielsen, arXiv:1805.05227.
[19] R. Harper and S. Flammia, arXiv:1806.02359.
[20] See Supplemental Material at http://link.aps.org/supplemental/10.1103/PhysRevLett.121.220502 for additional details, which includes Refs. [21–35].
[21] D. Gottesman, arXiv:1610.03507.
[22] T. Proctor, K. Rudinger, K. Young, M. Sarovar, and R. Blume-Kohout, Phys. Rev. Lett. **119**, 130502 (2017).
[23] A. W. Cross, L. S. Bishop, J. A. Smolin, and J. M. Gambetta, arXiv:1707.03429.
[24] IBM QX team, ibmqx4 backend specification (2017), https://github.com/Qiskit/ibmq-device-information/tree/master/backends/tenerife/V1.
[25] IBM QX team, ibmqx5 backend specification (2017), https://github.com/Qiskit/ibmq-device-information/tree/master/backends/rueschlikon/V1.
[26] R. S. Smith, M. J. Curtis, and W. J. Zeng, arXiv:1608.03355.
[27] Rigetti, The rigetti qpu (2018), https://www.rigetti.com/qpu.
[28] Rigetti (private communication).
[29] B. Efron, *Breakthroughs in Statistics* (Springer, New York, NY, 1992), p. 569.
[30] M. O. Scully and M. S. Zubairy, *Quantum Optics* (Cambridge University Press, Cambridge, England, 1997).
[31] D. A. Lidar, P. Zanardi, and K. Khodjasteh, Phys. Rev. A **78**, 012308 (2008).
[32] K. Khodjasteh and D. A. Lidar, Phys. Rev. A **75**, 062310 (2007).
[33] A. Uhlmann, Rep. Math. Phys. **9**, 273 (1976).
[34] G. Quiroz and D. A. Lidar, Phys. Rev. A **88**, 052306 (2013).
[35] T. Gullion, D. B. Baker, and M. S. Conradi, J. Magn. Reson. (1969) **89**, 479 (1990).
[36] L. Viola and S. Lloyd, Phys. Rev. A **58**, 2733 (1998).
[37] L.-M. Duan and G. Guo, Phys. Lett. A **261**, 139 (1999).
[38] P. Zanardi, Phys. Lett. A **258**, 77 (1999).
[39] L. Viola, E. Knill, and S. Lloyd, Phys. Rev. Lett. **82**, 2417 (1999).

[40] D. A. Lidar and T. A. Brun, *Quantum Error Correction* (Cambridge University Press, Cambridge, England, 2013).
[41] D. A. Lidar, Review of decoherence-free subspaces, noiseless subsystems, and dynamical decoupling, in *Quantum Information and Computation for Chemistry* (John Wiley & Sons, Inc., New York, 2014), p. 295.
[42] K. Khodjasteh and D. A. Lidar, Phys. Rev. Lett. **95**, 180501 (2005).
[43] G. S. Uhrig, Phys. Rev. Lett. **98**, 100504 (2007).
[44] J. R. West, B. H. Fong,, and D. A. Lidar, Phys. Rev. Lett. **104**, 130501 (2010).
[45] Z.-Y. Wang and R.-B. Liu, Phys. Rev. A **83**, 022306 (2011).
[46] K. Khodjasteh, D. A. Lidar, and L. Viola, Phys. Rev. Lett. **104**, 090501 (2010).
[47] A. M. Souza, G. A. Álvarez, and D. Suter, Phys. Rev. Lett. **106**, 240501 (2011).
[48] A. M. Souza, G. A. Álvarez, and D. Suter, Phil. Trans. R. Soc. A **370**, 4748 (2012).
[49] C. Kabytayev, T. J. Green, K. Khodjasteh, M. J. Biercuk, L. Viola, and K. R. Brown, Phys. Rev. A **90**, 012316 (2014).
[50] G. T. Genov, D. Schraft, N. V. Vitanov, and T. Halfmann, Phys. Rev. Lett. **118**, 133202 (2017).
[51] H. K. Ng, D. A. Lidar,, and J. Preskill, Phys. Rev. A **84**, 012305 (2011).
[52] J. Bylander, S. Gustavsson, F. Yan, F. Yoshihara, K. Harrabi, G. Fitch, D. Cory, Y. Nakamura, J. Tsai,, and W. Oliver, Nat. Phys. **7**, 565 (2011).
[53] G. A. Álvarez and D. Suter, Phys. Rev. Lett. **107**, 230501 (2011).
[54] M. Mukhtar, W. T. Soh, T. B. Saw, and J. Gong, Phys. Rev. A **82**, 052338 (2010).
[55] K. Khodjasteh and D. A. Lidar, Phys. Rev. A **68**, 022322 (2003); **72**, 029905(E) (2005).
[56] G. A. Paz-Silva and D. A. Lidar, Sci. Rep. **3**, 1530 (2013).